Appl. Phys. B 89, 483–488 (2007)
DOI: 10.1007/s00340-007-2867-4

Applied Physics B
Lasers and Optics

M. CHWALLA[1]
K. KIM[1]
T. MONZ[1]
P. SCHINDLER[1]
M. RIEBE[1]
C.F. ROOS[1,2,✉]
R. BLATT[1,2]

Precision spectroscopy with two correlated atoms

[1] Institut für Experimentalphysik, Universität Innsbruck, Technikerstraße 25, 6020 Innsbruck, Austria
[2] Institut für Quantenoptik und Quanteninformation der Österreichischen Akademie der Wissenschaften, Technikerstraße 21a, 6020 Innsbruck, Austria

Received: 22 June 2007/Revised version: 23 September 2007
Published online: 27 November 2007 •

ABSTRACT We discuss techniques that allow for long coherence times in laser spectroscopy experiments with two trapped ions. We show that for this purpose not only entangled ions prepared in decoherence-free subspaces can be used but also a pair of ions that are not entangled but subject to the same kind of phase noise. We apply this technique to a measurement of the electric quadrupole moment of the $3d^2D_{5/2}$ state of $^{40}Ca^+$ and to a measurement of the line width of an ultra-stable laser exciting a pair of $^{40}Ca^+$ ions.

PACS 03.67.-a; 06.30.Ft; 37.10.Ty

1 Introduction

Single trapped and laser-cooled ions are a nearly ideal system for high-resolution laser spectroscopy. The ion's internal as well as external quantum degrees of freedom can be controlled by coherent laser–atom interactions with high accuracy. At the same time, the ion is well isolated against detrimental influences of a decohering environment. The combination of these two properties have enabled spectacular ion trap experiments aiming at building better atomic clocks [1–4], creating entangled states [5, 6], and processing quantum information [7, 8]. The creation of multi-particle entangled atomic states is of interest in the context of quantum information processing but also for laser spectroscopy experiments. Maximally entangled states offer the prospect of improving the signal-to-noise ratio in precision spectroscopy experiments [9, 10] and they can be used to read out the quantum state of an atom by entangling it with another atom that is easier to detect [11]. Furthermore, in the state space of composite quantum systems made out of two or more atoms, it is sometimes possible to identify subspaces that are decoherence free [12] with respect to the dominant source of noise in the single-atom system [13]. It has been shown that such decoherence-free subspaces allow the preparation of entangled states of two ions with an entanglement lifetime of about one second predominantly limited by spontaneous decay of the involved metastable states [14]. These long entanglement lifetimes substantiate the usefulness of entangled states for precision measurements [15]. In [16] we applied this measurement technique to a pair of entangled $^{40}Ca^+$ ions for a precision measurement of the electric quadrupole moment of the $D_{5/2}$ state. The question arises of whether entanglement is an indispensable ingredient in these measurements. In this paper, we show that for a pair of correlated atoms coherence times exceeding the single-atom coherence times can be obtained even if the atoms are not entangled. The technique is applicable to measurements of energy-level shifts and transition frequencies in the presence of correlated noise. After a discussion of the measurement principle, we present two experiments applying the technique to a measurement of an electric quadrupole moment and to a determination of the line width of a narrow-band laser.

✉ Fax: +43 512 507 9816, E-mail: christian.roos@uibk.ac.at

2 Spectroscopy in decoherence-free subspaces

In atomic high-resolution spectroscopy, dephasing is often the most important factor limiting the attainable spectral resolution. Possible sources of dephasing are fluctuating electromagnetic fields giving rise to random energy-level shifts but also the finite spectral line width of probe lasers. Under these conditions, two atoms located in close proximity to each other are likely to experience the same kind of noise, i.e. they are subject to collective decoherence. The collective character of the decoherence has the important consequence that it does not affect the entangled two-atom state

$$\Psi_+ = \frac{1}{\sqrt{2}}(|g\rangle|e\rangle + |e\rangle|g\rangle)\,, \tag{1}$$

as both parts of the superposition are shifted by the same amount of energy by fluctuating fields. Here, for the sake of simplicity, $|g\rangle$ and $|e\rangle$ denote the ground and excited states of a two-level atom. Because of its immunity against collective decoherence, the entangled state Ψ_+ is much more robust than a single-atom superposition state $\frac{1}{\sqrt{2}}(|g\rangle + |e\rangle)$. This property makes states like Ψ_+ interesting candidates for high-precision spectroscopy. In the following, we will first discuss how to use Bell states for the measurement of energy-level shifts. Then, it will be shown that certain unentangled two-atom states can have similar advantages over single-atom superposition states albeit at lower signal-to-noise ratio.

2.1 *Spectroscopy with entangled states*

In a Ramsey experiment, spectroscopic information is inferred from a measurement of the relative phase φ of the superposition state $\frac{1}{\sqrt{2}}(|g\rangle + \mathrm{e}^{\mathrm{i}\varphi}|e\rangle)$. The phase is measured by mapping the states $\frac{1}{\sqrt{2}}(|g\rangle \pm |e\rangle)$ to the measurement basis $\{|g\rangle, |e\rangle\}$ by means of a $\pi/2$ pulse. In close analogy, spectroscopy with entangled states is based on a measurement of the relative phase φ of the Bell state $\Psi_\varphi = \frac{1}{\sqrt{2}}(|g\rangle|e\rangle + \mathrm{e}^{\mathrm{i}\varphi}|e\rangle|g\rangle)$. Here, the phase is determined by applying $\pi/2$ pulses to both atoms followed by state detection. $\pi/2$ pulses with the same laser phase on both atoms map the singlet state $\frac{1}{\sqrt{2}}(|g\rangle|e\rangle - |e\rangle|g\rangle)$ to itself, whereas the triplet state $\frac{1}{\sqrt{2}}(|g\rangle|e\rangle + |e\rangle|g\rangle)$ is mapped to a state $\frac{1}{\sqrt{2}}(|g\rangle|g\rangle + \mathrm{e}^{\mathrm{i}\alpha}|e\rangle|e\rangle)$ with different parity. Therefore, measurement of the parity operator $\sigma_z^{(1)}\sigma_z^{(2)}$ yields information about the relative phase, since $\langle\sigma_z^{(1)}\sigma_z^{(2)}\rangle = \cos\varphi$. If the atomic transition frequencies are not exactly equal but differ by an amount δ, the phase will evolve as a function of time τ according to $\varphi(\tau) = \varphi_0 + \delta\tau$. Then, measurement of the phase- evolution rate provides information about the difference frequency δ. To keep the notation simple, it was assumed that in both atoms the same energy levels participated in the superposition state of (1). In general, this does not need to be the case and the phase evolution is given by $\varphi(\tau) = ((\omega_{\mathrm{A}_1} - \omega_{\mathrm{L}_1}) \pm (\omega_{\mathrm{A}_2} - \omega_{\mathrm{L}_2}))\tau$. Here, $\omega_{\mathrm{A}_{1,2}}$ denote the atomic transition frequencies of atom 1 and atom 2, and $\omega_{\mathrm{L}_{1,2}}$ are the laser frequencies used for exciting the corresponding transitions. The minus sign applies if in the Bell state the ground state of atom 1 is associated with an excited state of atom 2 and vice versa. If the Bell state is a superposition of both atoms being in the ground state or both in the excited state, the plus sign is appropriate.

2.2 *Spectroscopy with unentangled states of two atoms*

One may wonder whether entanglement is absolutely necessary for observing long coherence times in experiments with two atoms. In fact, it turns out that the kind of measurement outlined above is applicable even to completely unentangled atoms. If the atoms are initially prepared in the product state

$$\begin{aligned}\Psi_\mathrm{p} &= \frac{1}{2}(|g\rangle + |e\rangle) \otimes (|g\rangle + |e\rangle) \\ &= \frac{1}{\sqrt{2}}\Psi_+ + \frac{1}{2}|g\rangle|g\rangle + \frac{1}{2}|e\rangle|e\rangle\,, \end{aligned} \tag{2}$$

this state will quickly dephase under the influence of collective phase noise. The resulting mixed state

$$\varrho_\mathrm{p} = \frac{1}{2}|\Psi_+\rangle\langle\Psi_+| + \frac{1}{4}|gg\rangle\langle gg| + \frac{1}{4}|ee\rangle\langle ee| \tag{3}$$

appears to be composed of the entangled state Ψ_+ with a probability of 50% and the two states $|gg\rangle$ and $|ee\rangle$ with 25% probability each. If the state Ψ_+ is replaced by the density operator ϱ_p in the measurement procedure described in Sect. 2.1, the resulting signal will be the same apart from a 50% loss of contrast. The states $|g\rangle|g\rangle$ and $|e\rangle|e\rangle$ do not contribute to the signal, since they become equally distributed over all four basis states by the $\pi/2$ pulses preceding the state detection. Their only effect is to reduce the signal-to-noise ratio by adding quantum projection noise, since only half of the experiments effectively contribute to the signal.

3 Experimental setup

For our experiments, we confine strings of cold $^{40}\mathrm{Ca}^+$ ions in a linear ion trap. The radial confinement with trap frequencies of about $\omega_\perp = (2\pi)\,4$ MHz is produced by a radio-frequency quadrupole field oscillating at 23.5 MHz. The axial center-of-mass frequency ω_z is changed from 860 kHz to 1720 kHz by varying the trap's tip voltages from 500 to 2000 V. For these trapping parameters, the distance between two trapped $^{40}\mathrm{Ca}^+$ ions is between 3.9 μm and 6.2 μm. Figure 1 shows the lowest energy levels of $^{40}\mathrm{Ca}^+$, the most important feature being the metastable D states with a lifetime of about 1 s. The ions are Doppler cooled on the $S_{1/2} \leftrightarrow P_{1/2}$ transition. Sideband cooling on the $S_{1/2} \leftrightarrow D_{5/2}$ quadrupole transition can be used to prepare a vibrational mode of the ion string in its ground state. At the beginning of each experiment, the ions are initialized in a pure state by optical pumping. Coherent quantum state manipulation is achieved by laser pulses exciting a single ion on the $|S_{1/2}, m\rangle \leftrightarrow |D_{5/2}, m'\rangle$ quadrupole transition. The Ti:sapphire laser used for exciting the transition has a line width of below 50 Hz. Its strongly focused beam is rapidly switched from one ion to the next by an electro-optical deflector so that only one ion is interacting with the beam at a time. We discriminate between the quantum states $S_{1/2}$ and $D_{5/2}$ by scattering light on the $S_{1/2} \leftrightarrow P_{1/2}$ dipole transition and detecting the presence or absence of resonance fluorescence of the individual ions with a CCD camera. For the measurement of operator expectation values, the experiments are typically repeated one hundred times. A more detailed account of the experimental setup is given in [17].

4 Applications

The measurement technique based on two unentangled atoms can be used for frequency measurement as well as for the detection of energy-level shifts. In the following subsections, it will be applied to a measurement of magnetic field gradients, to a determination of atomic electric quadrupole shifts, and to a measurement of the laser line width of a narrow-band laser.

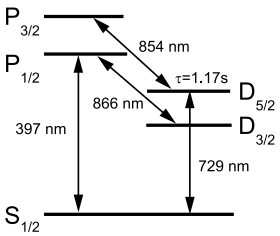

FIGURE 1 Relevant energy levels of $^{40}\mathrm{Ca}^+$. For Doppler cooling and quantum state detection, the ion is excited on the transitions $S_{1/2} \leftrightarrow P_{1/2} \leftrightarrow D_{3/2}$. Coherent operations are performed on the quadrupole transition to the long-lived $D_{5/2}$ state. Population in the $D_{5/2}$ state is pumped out via the $P_{3/2}$ level

4.1 *Detection of magnetic field gradients*

A magnetic field gradient pointing along the trap axis gives rise to Zeeman shifts that are different for all the ions. This is undesirable in experiments dedicated to quantum information processing as it would necessitate the use of different laser frequencies for performing the same type of operation on different ions. In order to compensate residual magnetic field gradients caused by the stray field of an ion getter pump and by asymmetrically placed magnetic field coils, we measured the magnetic field gradient by recording parity oscillations of a pair of ions prepared in the state given in (2) with $|g\rangle \equiv |S_{1/2}, m = 1/2\rangle$ and $|e\rangle \equiv |D_{5/2}, m = 5/2\rangle$. As in this experiment the Zeeman shift is the only relevant energy-level shift that is position dependent, the gradient was minimized by applying a compensation gradient and minimizing the parity oscillation frequency. For the chosen energy levels, the dependence of the transition frequency on the magnetic field is given by $\mathrm{d}\nu/\mathrm{d}B = 2.8\,\mathrm{MHz/G}$. Ramsey probe times of several hundred milliseconds make it possible to reduce the parity oscillation frequency to below 1 Hz. This corresponds to a difference of the magnetic fields at the location of the ions of less than 0.4 μG and to a field gradient of below 0.08 G/m if a typical ion distance of 5 μm is assumed. The precision of the measurement could be further increased by operating the ion trap at much lower axial trap frequencies in order to increase the distance between the ions.

4.2 *Measurement of electric quadrupole shifts*

In optical frequency standards based on single hydrogen-like trapped ions, the transition frequency from the S ground state to a metastable D_j state is sensitive to electric field gradients. The D_j state's atomic electric quadrupole moment interacting with residual electric quadrupole fields [18] gives rise to frequency shifts of a few hertz. The shift of the Zeeman sublevel $|D_j, m_j\rangle$ in a quadrupole field $\Phi(x, y, z) = A(x^2 + y^2 - 2z^2)$ with rotational symmetry is given by

$$\hbar\Delta\nu = \frac{1}{4}\frac{\mathrm{d}E_z}{\mathrm{d}z}\Theta(D, j)\frac{j(j+1) - 3{m_j}^2}{j(2j-1)}(3\cos^2\beta - 1)\,, \qquad (4)$$

where $\mathrm{d}E_z/\mathrm{d}z = 4A$ is the electric field gradient along the potential's symmetry axis z, β denotes the angle between the potential's symmetry axis $\vec{e}_z$ and the magnetic field vector $\vec{B}$, and the quantization axis z, and $\Theta(D, j)$ expresses the strength of the quadrupole moment in terms of a reduced matrix element [18]. Quadrupole moments have been calculated [19, 20] and experimentally determined [2, 21, 22] for $^{88}\mathrm{Sr}^+$, $^{199}\mathrm{Hg}^+$, and $^{171}\mathrm{Yb}^+$ by measuring the change in transition frequency from the electronic ground state to the metastable state that is affected by a static electric field gradient. In principle, the shift could also be detected by measuring transition frequencies between different Zeeman sublevels. However, both measurement strategies become impracticable in the presence of nonvanishing first-order Zeeman shifts since residual fluctuating magnetic fields prevent the use of sufficiently long laser–atom interaction times. In [16], we demonstrated that this problem can be overcome by preparing a pair of ions in an entangled state that is decoherence free with respect to fluctuations of the magnetic field but sensitive to the quadrupole shift. Figure 2 shows the energy-level shifts of the $D_{5/2}$ Zeeman sublevels under the influence of a magnetic field and an electric quadrupole field. Labeling the Zeeman states $|D_{5/2}, m\rangle \equiv |m\rangle$ by their magnetic quantum numbers, it can be seen that the Bell state

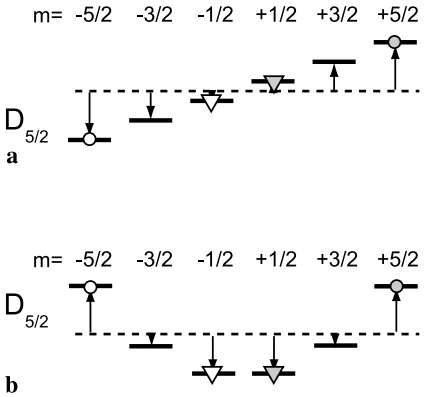

FIGURE 2 Shift of the Zeeman substates of the metastable $D_{5/2}$ level by (**a**) a magnetic field and (**b**) an electric field gradient. The magnetic quantum number is denoted by the symbol m. Energy levels occurring in the entangled state $\Psi_{\mathrm{ent}} = \frac{1}{\sqrt{2}}(|\circ\rangle|\bullet\rangle + |\triangledown\rangle|\blacktriangledown\rangle)$ and the product state $\Psi_{\mathrm{pr}} = \frac{1}{2}(|\circ\rangle + |\triangledown\rangle)(|\bullet\rangle + |\blacktriangledown\rangle)$ are denoted by the symbols $\circ, \triangledown, \bullet, \blacktriangledown$, the *open* (*filled*) *symbols* corresponding to levels occupied by atom 1 (2), respectively. The combined Zeeman energy of the $|\circ\rangle|\bullet\rangle$ states equals the energy of the $|\triangledown\rangle|\blacktriangledown\rangle$ states, making Ψ_{ent} immune against magnetic field noise. The Bell state and the product state used in the experiments (see (5) and (6)) have a slightly smaller sensitivity to the quadrupole shift than the states Ψ_{ent} and Ψ_{pr} but are easier to prepare

$$\Psi = \frac{1}{\sqrt{2}}(|-5/2\rangle|+3/2\rangle + |-1/2\rangle|-1/2\rangle) \qquad (5)$$

is a superposition of two constituents having energies that shift by the same amount in a magnetic field but shift in opposite directions if an electric field gradient is applied. We used this type of Bell state for a precise determination of the $D_{5/2}$ state's quadrupole moment in $^{40}\mathrm{Ca}^+$ [16].

To test whether the method outlined in Sect. 2.2 could be applied to a measurement of the quadrupole moment, we prepared the state

$$\Psi_{\mathrm{p}} = \frac{1}{2}(|-5/2\rangle + |-1/2\rangle) \otimes (|+3/2\rangle + |-1/2\rangle) \qquad (6)$$

and let the fluctuating magnetic stray fields turn the pure state into a mixed state within a few milliseconds. After a waiting time ranging from 0.1 to 200 ms, $\pi/2$ pulses were applied and a parity measurement performed. Figure 3 shows the resulting parity oscillations whose contrast decays over a time interval orders of magnitude longer than any single-atom coherence time in $^{40}\mathrm{Ca}^+$. A sinusoidal fit to the data reveals an initial contrast of 48(6)% and an oscillation frequency $\nu = 38.6(3)$ Hz. For the fit, the first data point at $t = 0.1$ μs is not taken into account. At this time, the quantum state cannot yet be described by a mixture similar to the one of (3) as some of the coherences persist for a few milliseconds and thus affect the parity signal. The parity signal decays exponentially with a time constant $\tau_{\mathrm{d}} = 730(530)$ ms that is consistent with the assumption of spontaneous decay

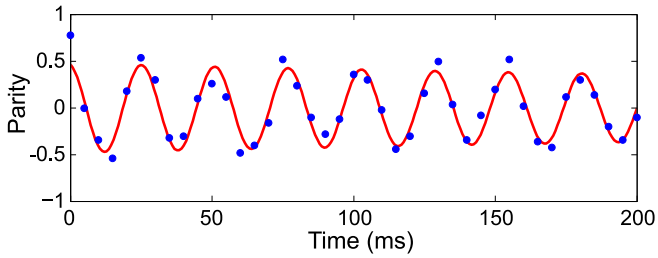

FIGURE 3 Parity oscillations caused by the interaction of a static electric field gradient with the quadrupole moment of the $D_{5/2}$ state of $^{40}Ca^{+}$. The quadrupole shift is inferred from the frequency of the parity oscillations. The first data point significantly deviates from the fit since the quantum state given by (6) has not yet decayed to a mixed quantum state. For the setting of the analysis pulses, the pure state gives a significantly higher value of the parity. Techniques similar to the ones later described in Sect. 4.3 could in principle be used to avoid this complication

being the only source of decoherence (in this case, one would have $\tau_d = \tau_{D_{5/2}}/2 \approx 580$ ms, where $\tau_{D_{5/2}}$ is the lifetime of the metastable state). The quadrupole moment is determined by measuring the quadrupole shift as a function of the electric field gradient E'. The latter is conveniently varied by changing the voltage applied to the axial trap electrodes. For a calibration of the gradient, the axial oscillation frequency of the ions is measured. Further details regarding the measurement procedure are provided in [16]. Figure 4a shows the quadrupole shift $\Delta\nu_{QS}$ as a function of the field gradient (the small offset at $E' = 0$ is caused by the second-order Zeeman effect). By fitting a straight line to the data, the quadrupole moment can be calculated provided that the angle between the orientation of the electric field gradient and the quantization axis is known. Setting $\Delta\nu_{QS} = \alpha E'$, the fit yields the proportionality constant $\alpha = 2.977(11)$ Hz/(V/mm^2). For the same configuration, the quadrupole shift was also measured with an entangled state, giving $\alpha = 2.975(2)$ Hz/(V/mm^2) and thus confirming that the measurements with product and with entangled states give the same result. Figure 4b shows the deviations of the data points measured with entangled and with classically correlated ions with respect to the fit obtained from the entangled state data. As expected, the error bars of the measurement with classically correlated ions are bigger since the Ramsey contrast is reduced and the quantum projection noise is higher. A rough estimation of the influence of quantum projection noise on the uncertainty σ of the quadrupole shift $\Delta\nu_{QS}$ is obtained by setting $\sigma_{\Delta\nu_{QS}} \backsimeq 1/((\tau/2)(C\sqrt{2N}))$, where τ is the maximum delay between state preparation and parity measurement, C the resulting Ramsey contrast, and N denotes the number of experiments (for two ions, $2N$ state measurements contribute to the signal). For the experiments with entangled states shown in Fig. 4b, where $N \approx 30\,000$, $C \approx 0.5$, and $\tau = 250$ ms, one expects $\sigma_{\Delta\nu_{QS}} \approx 65$ mHz. For the product state experiments ($N \approx 20\,000$, $C \approx 0.3$, $\tau = 100$ ms), one expects $\sigma_{\Delta\nu_{QS}} \approx 330$ mHz. These estimates are consistent with the experimental observations. Even though experiments with product states suffer from a reduced Ramsey contrast, they are attractive because these experiments are considerably easier to realize. Contrary to the ones based on entangled states, they do not require cooling the ions to the ground state of the trapping potential by sideband cooling on the quadrupole transition using a laser with a narrow line width. Moreover, it turns out that the precision of the quadrupole moment measurement is not limited by the statistical errors but rather by a number of systematic errors, the most important one being the alignment of the magnetic field vector defining the quantization axis with the symmetry axis of the trap [16] described by the angle β in (4). As can be seen from (4), any misalignment will reduce the quadrupole shift and thus result in an underestimation of the quadrupole moment. In [16], the precision of the measurement was limited by the estimated uncertainty of $\Delta\beta = 3°$.

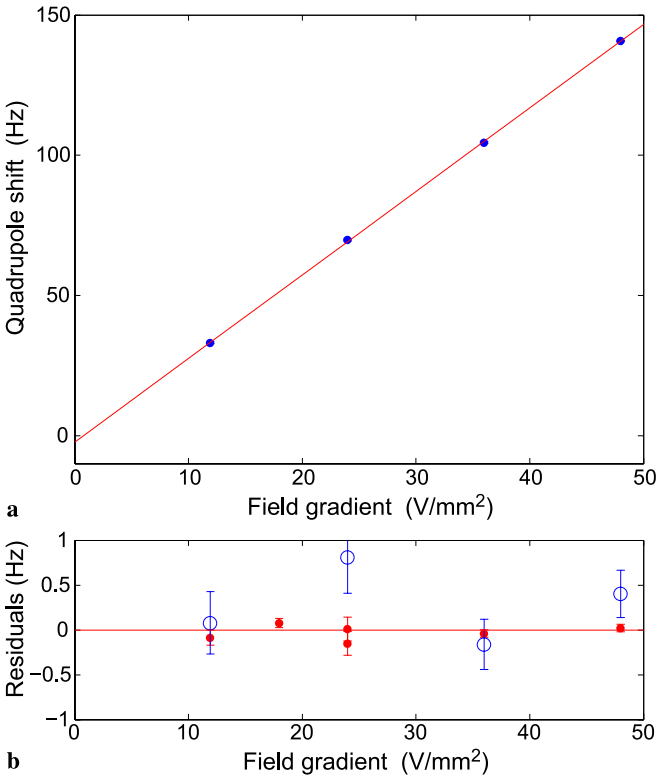

FIGURE 4 Electric quadrupole shift measured with a pair of atoms in a product state. (**a**) The shift varies linearly with the applied electric field gradient. (**b**) Residuals of the electric quadrupole shift measurements. The plot shows deviations of the data points measured with unentangled ions (*open circles*) and entangled ions (*filled circles*) with respect to the fit obtained from the entangled state data. For the measurement with product states (entangled states), $N \approx 20\,000$ ($N \approx 30\,000$) states were prepared, waiting times of up to 100 ms (250 ms) were used, and the overall time of data taking was 6 (9) h, respectively

4.3 *Laser line width measurements*

The line width of a narrow-band laser is often investigated by setting up two identical laser systems and observing their beat signal. If no second laser system is available, Ramsey experiments are a suitable tool for determining the laser line width [23]. This, however, requires the atomic transition line width not to be broadened by phase noise to an extent comparable to the laser line width to be measured. In $^{40}Ca^{+}$, this requirement is difficult to fulfill for lasers with a line width of 100 Hz or below as all transitions depend on the magnetic field in first order. Here again, a solution consists in performing Ramsey measurements with a pair of ions in a correlated product state. For a measurement of the line

width of the Ti:sapphire laser exciting the $^{40}Ca^{+}$ ions on the $S_{1/2} \leftrightarrow D_{5/2}$ transition, we prepared the state $\Psi_p = \psi_1 \otimes \psi_2$, where

$$\psi_1 = \frac{1}{\sqrt{2}}(|S_{1/2}, m = -1/2\rangle + |D_{5/2}, m = -1/2\rangle)\,,$$
$$\psi_2 = \frac{1}{\sqrt{2}}(|S_{1/2}, m = +1/2\rangle + |D_{5/2}, m = +1/2\rangle)$$

denote the states of ion 1 and ion 2. The fringes of the single-ion Ramsey signals $\langle\sigma_z^{(n)}\rangle = \cos(\varphi_L + (-1)^n\varphi_B + \varphi_n)$, $n = 1, 2$, show the same dependence on changes of the laser frequency but shift in opposite directions under changes of the magnetic field. Here, φ_L is the phase shift arising from deviations of the laser frequency from the atomic transition frequency, φ_B denotes shifts due to deviations of the magnetic field from its mean value, and φ_n is the phase difference between the first and the second Ramsey pulses. Then, the two-ion parity signal is given by

$$\begin{aligned}\left\langle\sigma_z^{(1)}\sigma_z^{(2)}\right\rangle &= \langle\cos(\varphi_L - \varphi_B + \varphi_1)\cos(\varphi_L + \varphi_B + \varphi_2)\rangle \\ &= \frac{1}{2}(\langle\cos(2\varphi_L + \varphi_2 + \varphi_1)\rangle + \langle\cos(2\varphi_B + \varphi_2 - \varphi_1)\rangle).\end{aligned} \tag{7}$$

In the parity signal, the phase noise contributions from the laser and the magnetic field separate. Moreover, it is even possible to make either the first or the second term vanish by the following procedure: for an estimation of the expectation value of the observable $\sigma_z^{(1)}\sigma_z^{(2)}$, a Ramsey experiment is carried out N times. If the phases φ_1, φ_2 are chosen to be random variables by setting $\varphi_1 = \varphi_0 + \varphi_X$, $\varphi_2 = -\varphi_X$, where φ_X is a random variable with uniform distribution over the interval $[0, 2\pi)$, the magnetic-field-dependent term averages to zero and (7) becomes

$$\left\langle\sigma_z^{(1)}\sigma_z^{(2)}\right\rangle = \frac{1}{2}\langle\cos(2\varphi_L + \varphi_0)\rangle\,, \tag{8}$$

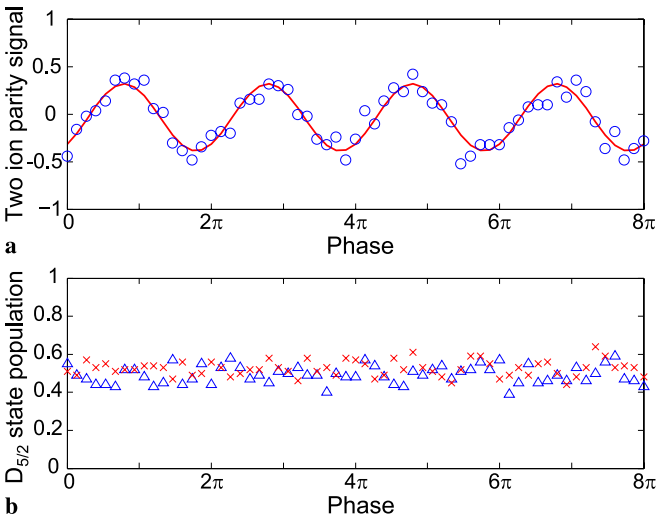

FIGURE 5 Two-ion Ramsey experiment for a measurement of the laser line width. (**a**) Two-ion parity signal measured as a function of φ_0 for a Ramsey time $\tau = 1.51$ ms. (**b**) Single-ion coherences. Because of the randomization of the second pulses' phase with respect to the phase of the first pulse, the signal is completely flat

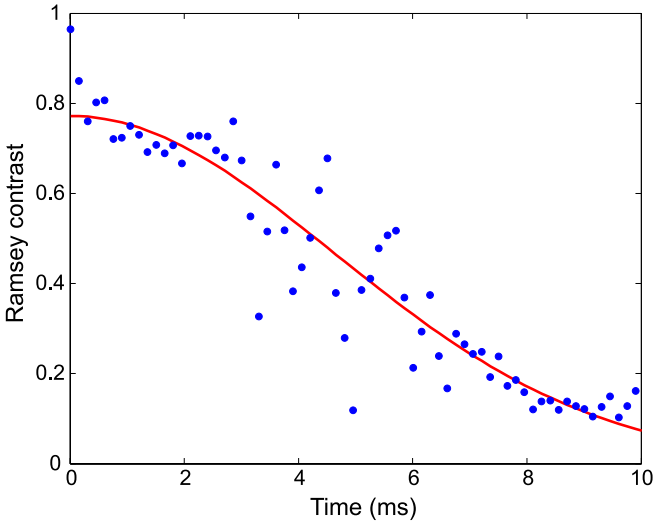

FIGURE 6 Measurement of the laser line width by a two-ion Ramsey experiment. The Ramsey contrast as a function of time is fitted by a Gaussian with half-width $\tau_{1/2} = 4.6(2)$ ms

as only the sum $\varphi_1 + \varphi_2 = \varphi_0$ is not a random number. By setting $\varphi_1 = \varphi_0 + \varphi_X$, $\varphi_2 = \varphi_X$, the experiment could also be made sensitive to decoherence caused by magnetic field noise and insensitive to laser frequency noise. In both cases, all single-ion coherences are completely averaged out. By scanning the phase φ_0, Ramsey fringes are recorded for the parity $\sigma_z^{(1)}\sigma_z^{(2)}$ and the resulting Ramsey contrast can be plotted as a function of the Ramsey time. Note that the Ramsey contrast will decay twice as fast as in a standard Ramsey experiment with a single atom because of the factor $2\varphi_L$ in (7).

Ramsey fringes recorded by this technique are shown in Fig. 5. The figure's upper panel displays the two-ion parity signal as a function of φ_0 for a Ramsey time $\tau = 1.51$ ms. The lower panel shows the single-ion signals $\langle\sigma_z^{(1)}\rangle$, $\langle\sigma_z^{(2)}\rangle$, having no contrast at all. In Fig. 6, the two-ion Ramsey contrast is plotted as a function of the Ramsey time τ. As low-frequency laser noise is the dominant source of noise broadening the laser line width in our experiments, the Ramsey contrast data are fitted by a Gaussian function with a half-width $\tau_{1/2} = 4.6(2)$ ms. From this value, we infer a laser line width of 48(2) Hz on a time scale of 1 min.

5 Conclusions

In ion-trap experiments, one is often confronted with collective decoherence mechanisms caused by external fluctuating fields with spatial correlation lengths much longer than the typical distance between ions. In these conditions, experiments with correlated ions prepared in decoherence-free subspaces allow for substantially longer coherence times than experiments investigating single-ion coherences only. While the preparation of entangled states is optimum for achieving high signal-to-noise ratios, substantial improvements can already be achieved by experimenting with ions that are classically correlated but not entangled.

ACKNOWLEDGEMENTS We acknowledge support by the Austrian Science Fund (FWF), the European Commission (SCALA, CONQUEST networks), and the Institut für Quanteninformation GmbH.

K.K. acknowledges funding by the Lise Meitner program of the FWF. C.F.R. would like to thank Bodensteinalm for hospitality during the last stage of the preparation of the manuscript.

REFERENCES

1 H.S. Margolis, G.P. Barwood, G. Huang, H.A. Klein, S.N. Lea, K. Szymaniec, P. Gill, Science **306**, 1355 (2004)
2 T. Schneider, E. Peik, C. Tamm, Phys. Rev. Lett. **94**, 230 801 (2005)
3 W.H. Oskay, S.A. Diddams, E.A. Donley, T.M. Fortier, T.P. Heavner, L. Hollberg, W.M. Itano, S.R. Jefferts, M.J. Delaney, K. Kim, F. Levi, T.E. Parker, J.C. Bergquist, Phys. Rev. Lett. **97**, 020 801 (2006)
4 T. Rosenband, P.O. Schmidt, D.B. Hume, W.M. Itano, T.M. Fortier, J.E. Stalnaker, K. Kim, S.A. Diddams, J.C.J. Koelemeij, J.C. Bergquist, D.J. Wineland, Phys. Rev. Lett. **98**, 220 801 (2007)
5 D. Leibfried, E. Knill, S. Seidelin, J. Britton, R.B. Blakestad, J. Chiaverini, D.B. Hume, W.M. Itano, J.D. Jost, C. Langer, R. Ozeri, R. Reichle, D.J. Wineland, Nature **438**, 639 (2005)
6 H. Häffner, W. Hänsel, C.F. Roos, J. Benhelm, D. Chek-al-kar, M. Chwalla, T. Körber, U.D. Rapol, M. Riebe, P.O. Schmidt, C. Becher, O. Gühne, W. Dür, R. Blatt, Nature **438**, 643 (2005)
7 M. Riebe, H. Häffner, C.F. Roos, W. Hänsel, J. Benhelm, G.P.T. Lancaster, T.W. Körber, C. Becher, F. Schmidt-Kaler, D.F.V. James, R. Blatt, Nature **429**, 734 (2004)
8 M.D. Barrett, J. Chiaverini, T. Schätz, J. Britton, W.M. Itano, J.D. Jost, E. Knill, C. Langer, D. Leibfried, R. Ozeri, D.J. Wineland, Nature **429**, 737 (2004)
9 J.J. Bollinger, W.M. Itano, D.J. Wineland, D.J. Heinzen, Phys. Rev. A **54**, R4649 (1996)
10 D. Leibfried, M.D. Barrett, T. Schätz, J. Britton, J. Chiaverini, W.M. Itano, J.D. Jost, C. Langer, D.J. Wineland, Science **304**, 1476 (2004)
11 P.O. Schmidt, T. Rosenband, C. Langer, W.M. Itano, J.C. Bergquist, D.J. Wineland, Science **309**, 749 (2005)
12 D.A. Lidar, I.L. Chuang, K.B. Whaley, Phys. Rev. Lett. **81**, 2594 (1998)
13 D. Kielpinski, V. Meyer, M.A. Rowe, C.A. Sackett, W.M. Itano, C. Monroe, D.J. Wineland, Science **291**, 1013 (2001)
14 C.F. Roos, G.P.T. Lancaster, M. Riebe, H. Häffner, W. Hänsel, S. Gulde, C. Becher, J. Eschner, F. Schmidt-Kaler, R. Blatt, Phys. Rev. Lett. **92**, 220402 (2004)
15 C.F. Roos, arXiv:quant-ph/0508148 (2005)
16 C.F. Roos, M. Chwalla, K. Kim, M. Riebe, R. Blatt, Nature **443**, 316 (2006)
17 F. Schmidt-Kaler, H. Häffner, S. Gulde, M. Riebe, G.P.T. Lancaster, T. Deuschle, C. Becher, W. Hänsel, J. Eschner, C.F. Roos, R. Blatt, Appl. Phys. B **77**, 789 (2003)
18 W.M. Itano, J. Res. Natl. Inst. Stand. Technol. **105**, 829 (2000)
19 W.M. Itano, Phys. Rev. A **73**, 022510 (2006)
20 C. Sur, K.V.P. Latha, B.K. Sahoo, R.K. Chaudhuri, B.P. Das, Phys. Rev. Lett. **96**, 193001 (2006)
21 W.H. Oskay, W.M. Itano, J.C. Bergquist, Phys. Rev. Lett. **94**, 163001 (2005)
22 G.P. Barwood, H.S. Margolis, G. Huang, P. Gill, H.A. Klein, Phys. Rev. Lett. **93**, 133001 (2004)
23 K. Sengstock, U. Sterr, J.H. Müller, V. Rieger, D. Bettermann, W. Ertmer, Appl. Phys. B **59**, 99 (1994)